TEL AVIV UNIVERSITY
Pursuing the Unknown

Deeply virtual pion production analysis in RG-A

Igor Korover

CLAS Collaboration November 2025

Exclusive deeply virtual π^oelectroproduction

$$ep \to e'p'\pi^0$$

At **large** Q^2 and W with fixed x_B and $|t| \ll Q^2$ Should factorize into GPDs and hard scattering subprocess.

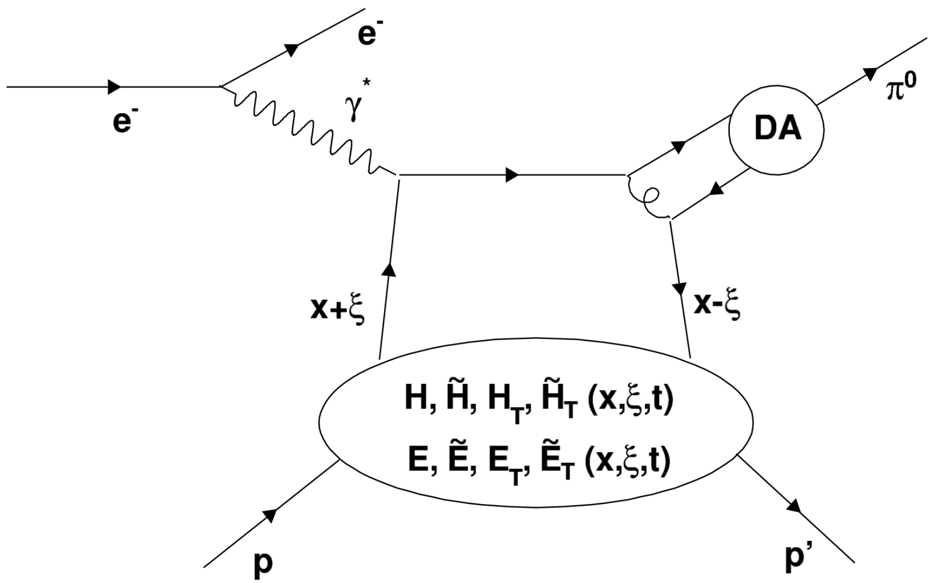

J.C. Collins, L. Frankfurt, and M. Strikman

σ_L – dominant
σ_T– supressed by $1/Q^2$

$$\boxed{\begin{array}{l}\sigma_L \sim \dfrac{1}{Q^6} \\ \dfrac{\sigma_T}{\sigma_L} \sim \dfrac{1}{Q^2} \\ Q^2 \to \infty\end{array}} \; x_B, t \ fixed$$

Not observed at accesible Q^2

Transversity GPD model:

- Goloskokov and Kroll
- Liuti and Goldstein

$$\sigma_L \ll \sigma_T$$

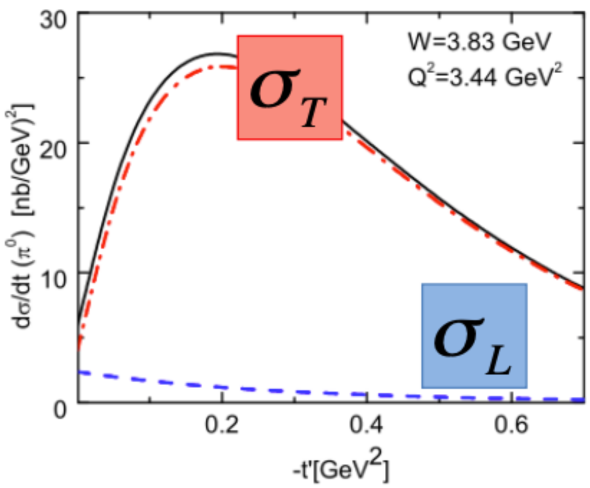

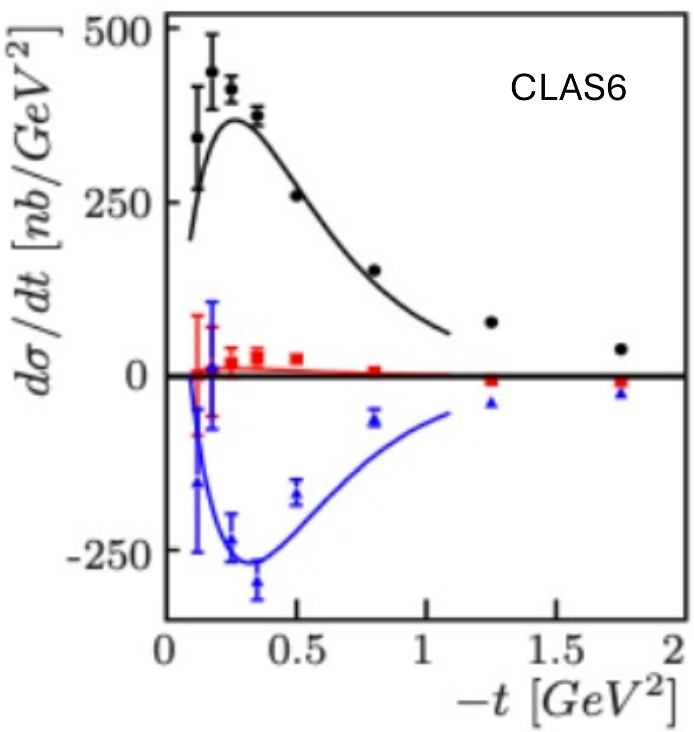

$$\frac{d^2\sigma}{dt\,d\phi_\pi} = \frac{1}{2\pi}\left[\left(\frac{d\sigma_T}{dt} + \epsilon\frac{d\sigma_L}{dt}\right) + \epsilon\cos 2\phi_\pi \frac{d\sigma_{TT}}{dt} + \sqrt{2\epsilon(1+\epsilon)}\cos\phi_\pi \frac{d\sigma_{LT}}{dt}\right].$$

<u>Structure functions and GPDs</u>

$$\frac{d\sigma_L}{dt} = \frac{4\pi\alpha}{kQ^2}\left\{(1-\xi^2)\,|\langle\tilde{H}\rangle|^2 - 2\xi^2\Re\left[\langle\tilde{H}\rangle^*\langle\tilde{E}\rangle\right] - \frac{t'}{4m^2}\xi^2|\langle\tilde{E}\rangle|^2\right\}$$

$$\frac{d\sigma_T}{dt} = \frac{2\pi\alpha\mu_\pi^2}{kQ^4}\left\{(1-\xi^2)\,|\langle H_T\rangle|^2 - \frac{t'}{8m^2}|\langle\bar{E}_T\rangle|^2\right\}$$

$$\frac{d\sigma_{LT}}{dt} = \frac{4\pi\alpha\mu_\pi}{\sqrt{2}kQ^3}\xi\sqrt{1-\xi^2}\,\frac{\sqrt{-t'}}{2m}\Re\left\{\langle H_T\rangle^*\langle\tilde{E}\rangle\right\}$$

$$\frac{d\sigma_{TT}}{dt} = \frac{4\pi\alpha\mu_\pi^2}{kQ^4}\,\frac{-t'}{16m^2}\langle\bar{E}_T\rangle^2$$

Experimental extraction of differential cross section

Under the assumption of single photon exchange: $ep \rightarrow e'p'\pi^0$

$$\frac{d^4\sigma}{dQ^2 dx_B dt d\phi_\pi} = \Gamma(Q^2, x_B, E)\frac{1}{2\pi}\left[\left(\frac{d\sigma_T}{dt} + \epsilon\frac{d\sigma_L}{dt}\right) + \epsilon\cos 2\phi_\pi \frac{d\sigma_{TT}}{dt} + \sqrt{2\epsilon(1+\epsilon)}\cos\phi_\pi \frac{d\sigma_{LT}}{dt}\right]$$

Virtual photon flux:

$$\Gamma(Q^2, x_B, E) = \frac{\alpha}{8\pi}\frac{Q^2}{m_p^2 E^2}\frac{1-x_B}{x_B^3}\frac{1}{1-\epsilon}$$

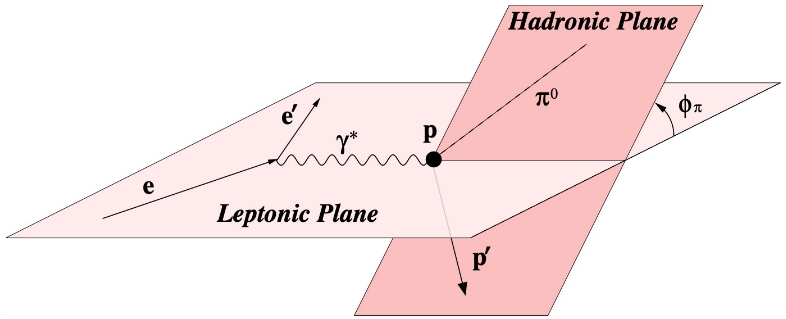

$$\frac{d^4\sigma}{dQ^2\, dx_B\, dt\, d\phi_\pi} = \frac{N(Q^2, x_B, t, \phi_\pi)}{\mathcal{L}_{\rm int}\, \Delta Q^2\, \Delta x_B\, \Delta t\, \Delta\phi_\pi} \cdot \frac{1}{\epsilon_{\rm acc}\, \delta_{\rm RC}\, \delta_{\rm Norm}\, Br(\pi^0 \rightarrow \gamma\gamma)}$$

Main goal of the analysis is to extract the structure functions over wide phase space

$$\frac{d\sigma_U}{dt}$$

$$\frac{d\sigma_{LT}}{dt}$$

Main avantage: the dynamics in $Q^2, x_B, -t$

less sensitive to global normalization

$$\frac{d\sigma_{TT}}{dt}$$

$\sigma_U = (\sigma_T + \epsilon\sigma_L)$

RGA – 10.6 GeV electron beam

Two magnet configurations:
- Inbending
- Outbending

Advantage:
Wider coverage and cross check for overlaping kinematic bins

Deeply virtual process

$$Q^2 > 1\ GeV^2$$

$$W > 2\ GeV$$

$$p_e > 2\ GeV$$

Phase space Q^2, x_B

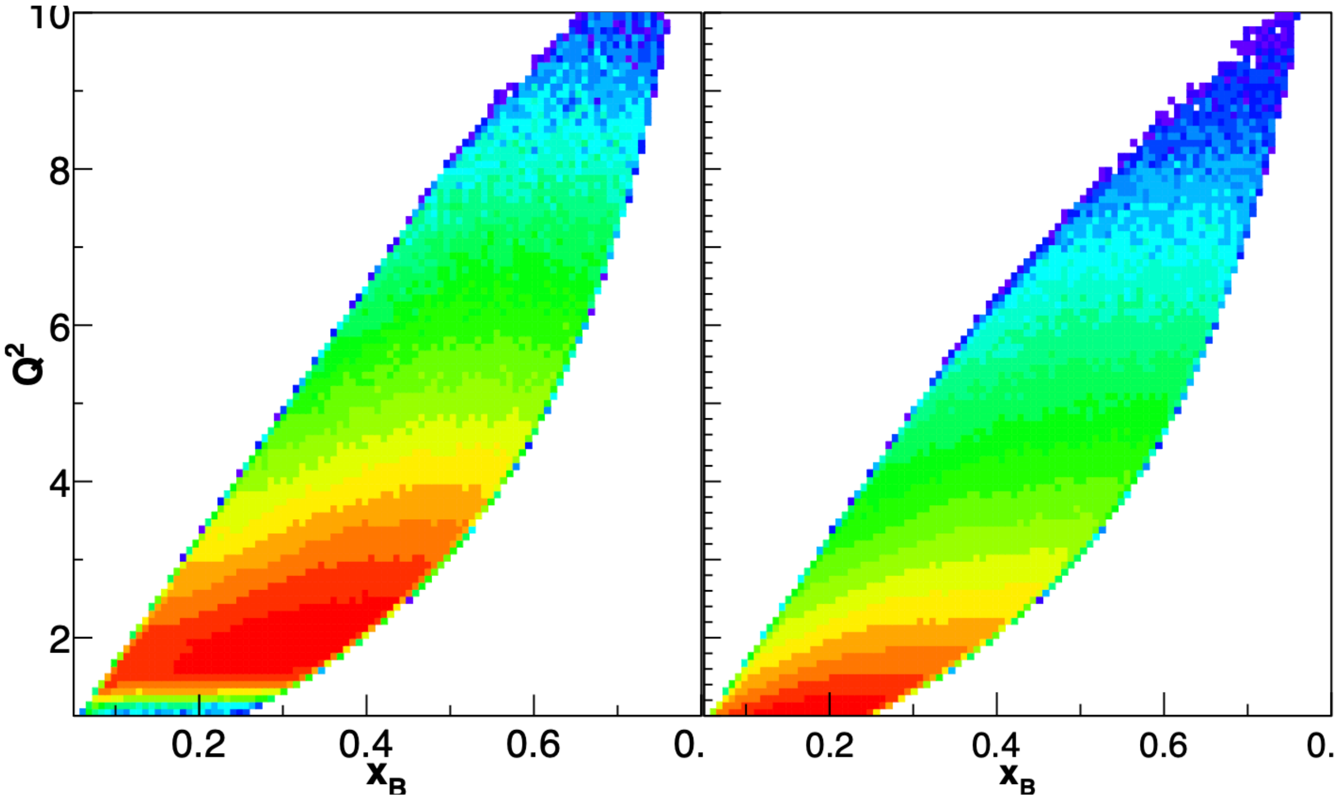

Fully exclusive reactions:

Detection of all particle participating in the proces:

- Scattered electron
- Proton
- Neutral pion via detection of 2 high energy photons

Electron detection

Only in Forward detector

Proton

Forward or Central detectors

Two photons

Forward detector or
Forward tagger

Selection of scattering electron is based on standard PID

Sampling fraction

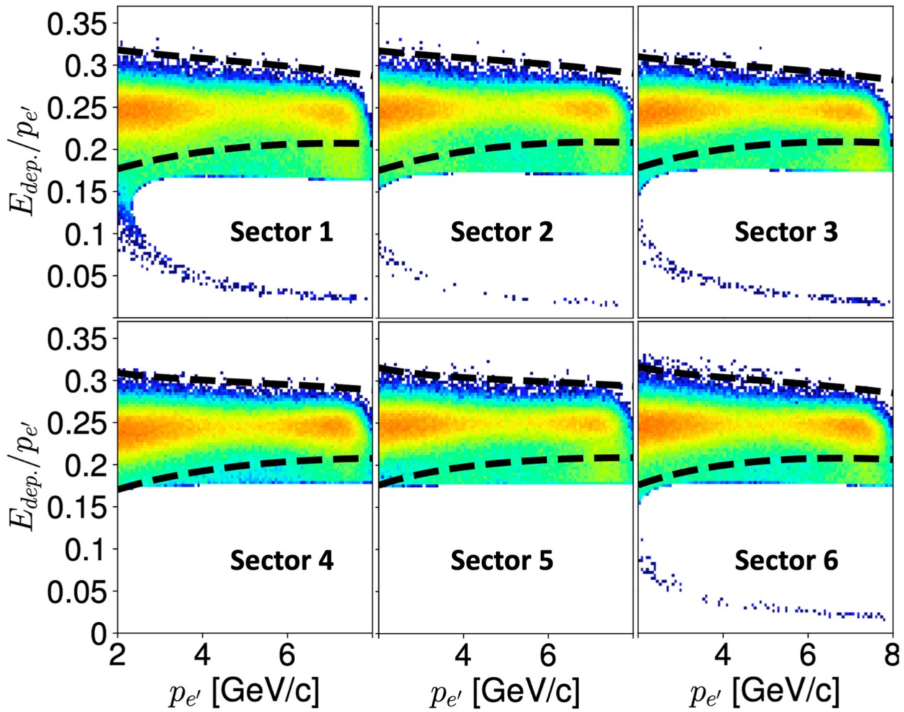

Cuts used for common analysis.

Drift chambers

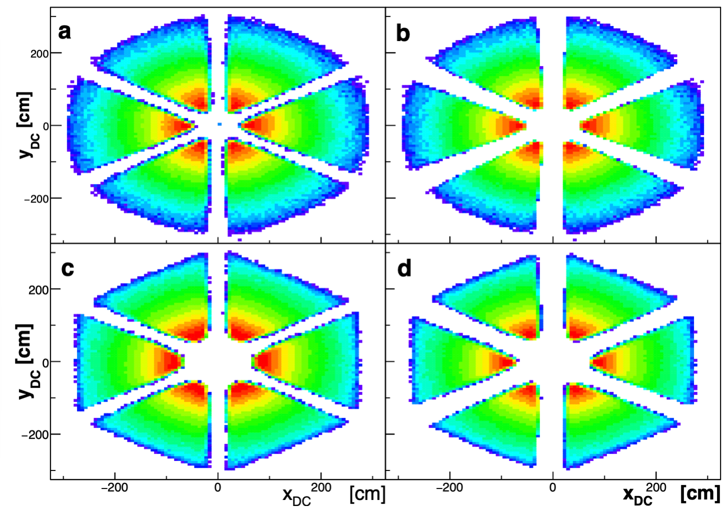

EM callorimeter

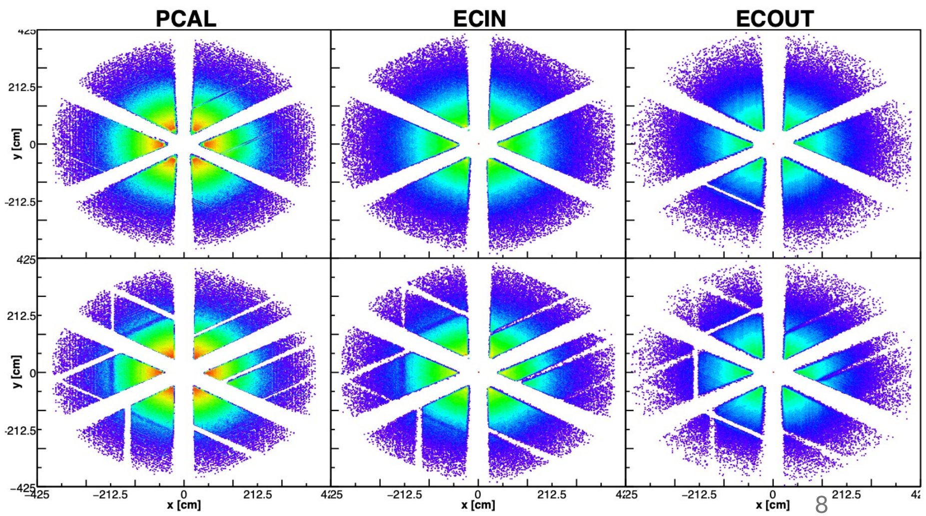

Protons:

Cuts used for common analysis pass-1 with modifications:

- Recent approved DVCS note from RGA.
- New common analysis pass-2 note (to be submitted).

Drift chamber

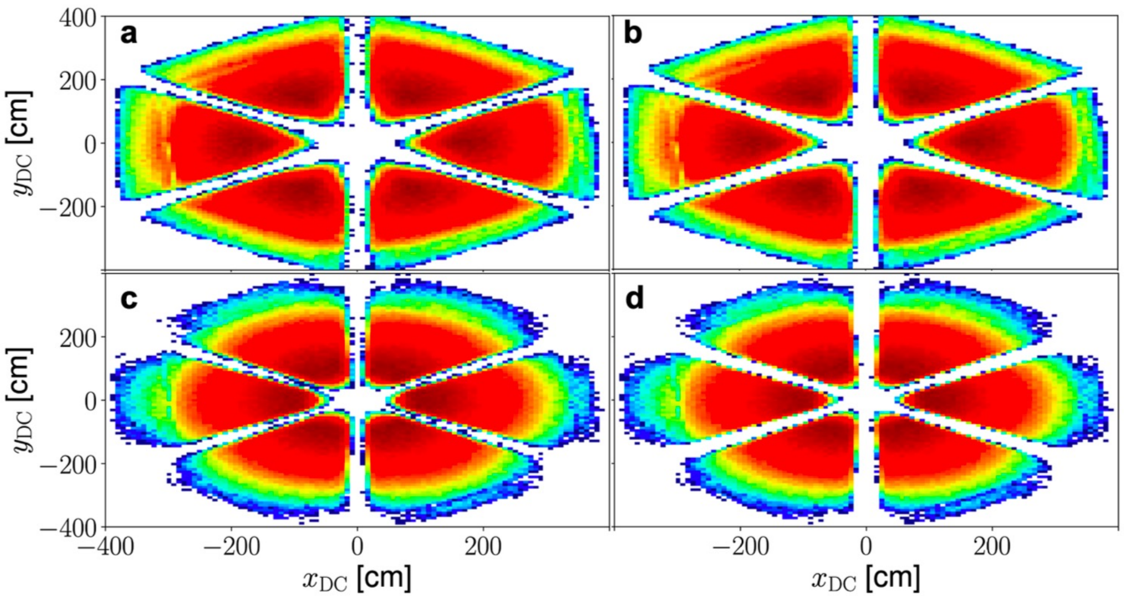

CVT

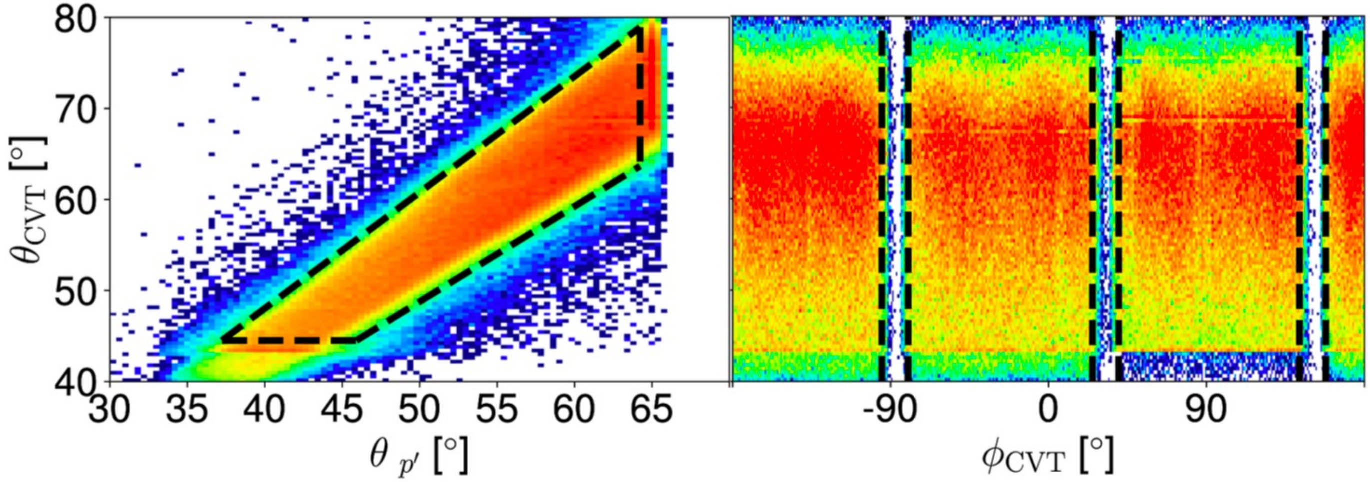

Photons

EM

Similar to electron case, exclusion of dead regions

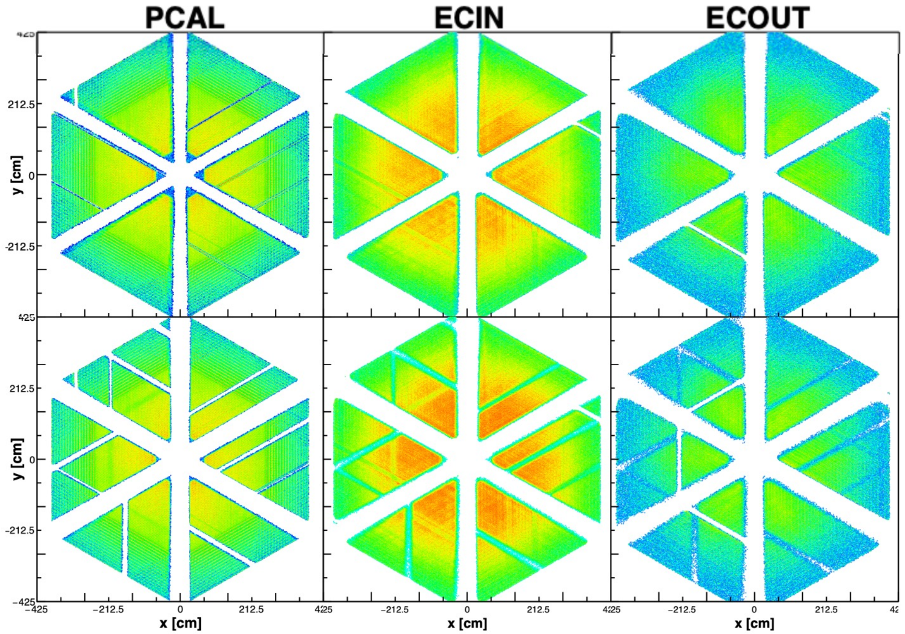

Forward tagger

Exclusing “holes” in FT

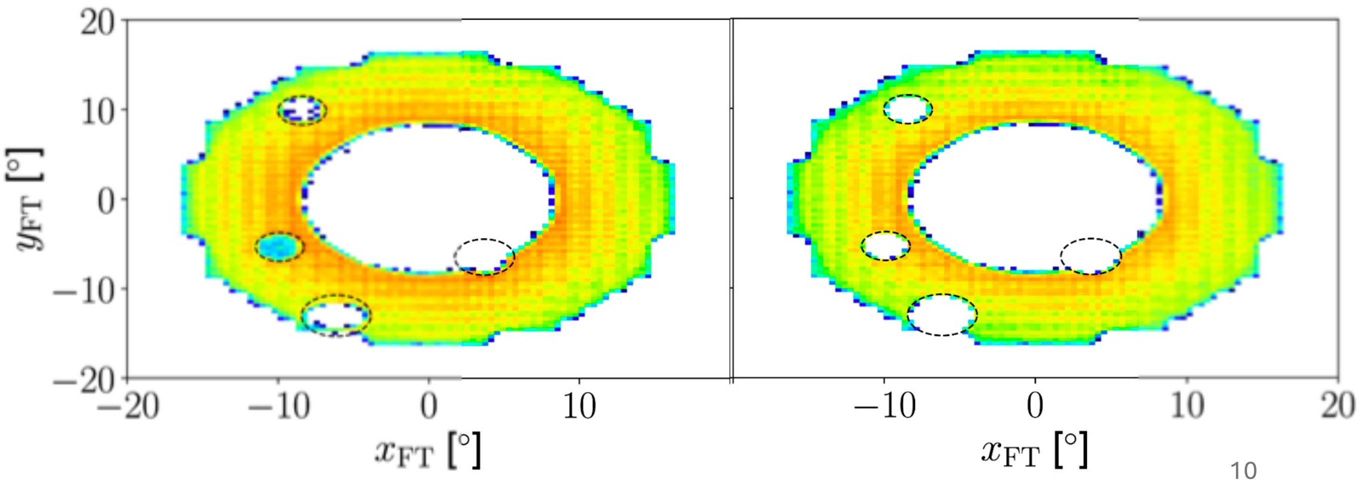

Momentum corrections

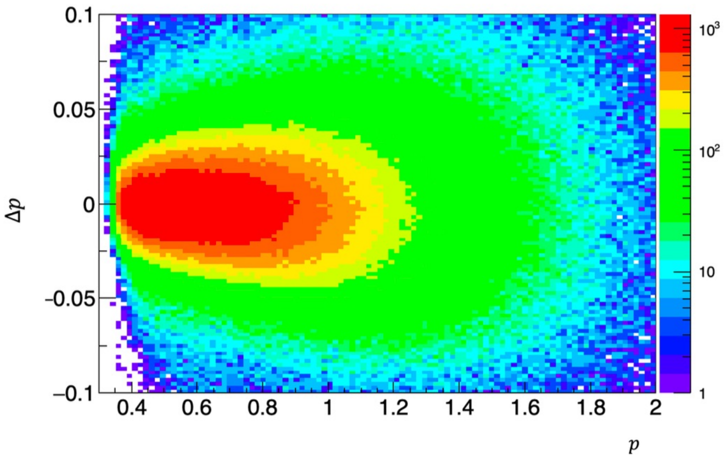

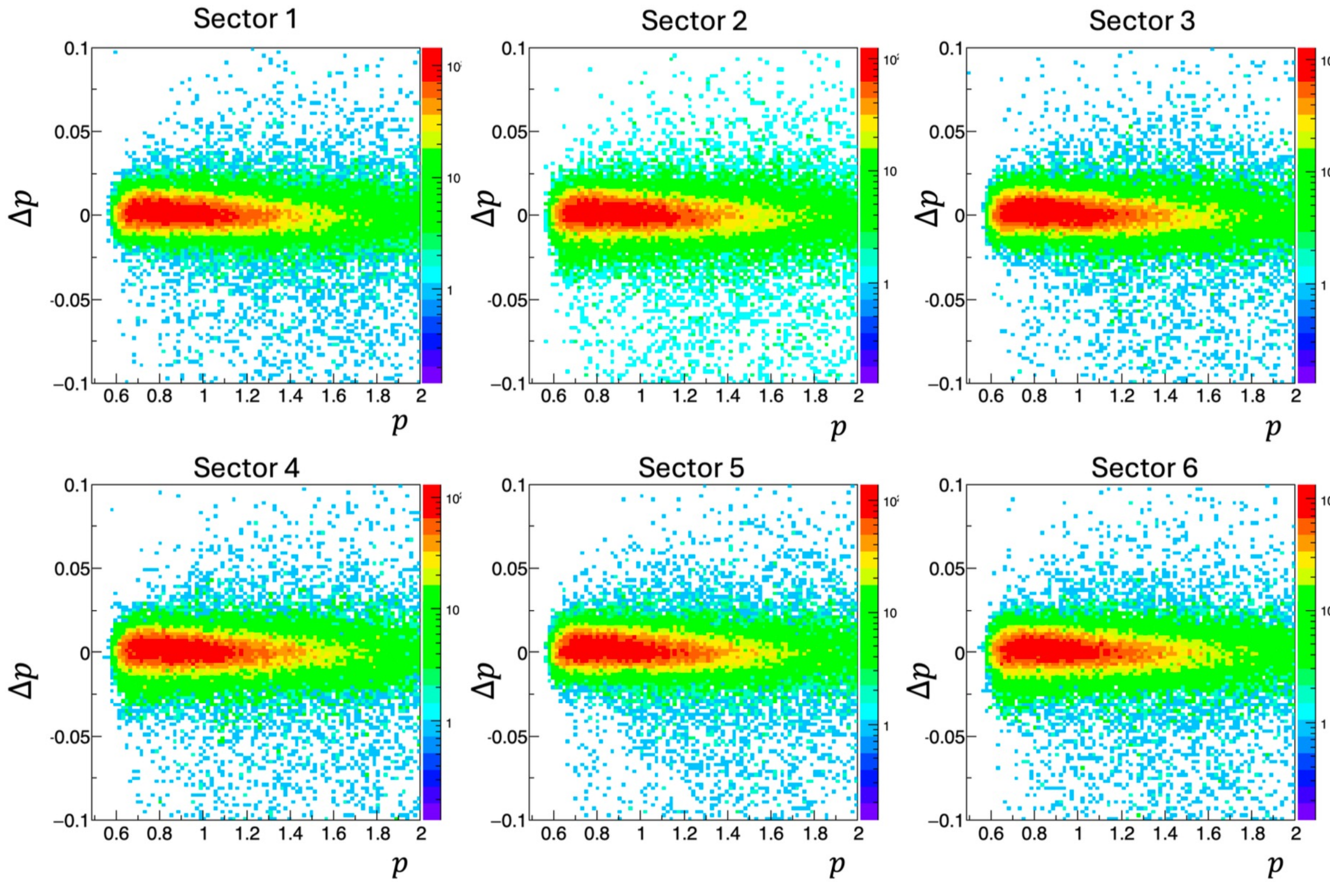

$$p_{\mathrm{corr}} = p_{\mathrm{rec}} \ + \ A_p(\theta) \ + \ \frac{B_p(\theta)}{p_{\mathrm{rec}}} \ + \ \frac{C_p(\theta)}{p_{\mathrm{rec}}^2}$$

Will be reported in common pass-2 analysis note.

Neutral pion selection

Invariant mass of $\gamma\gamma$ system

*After exclusivity selection cuts

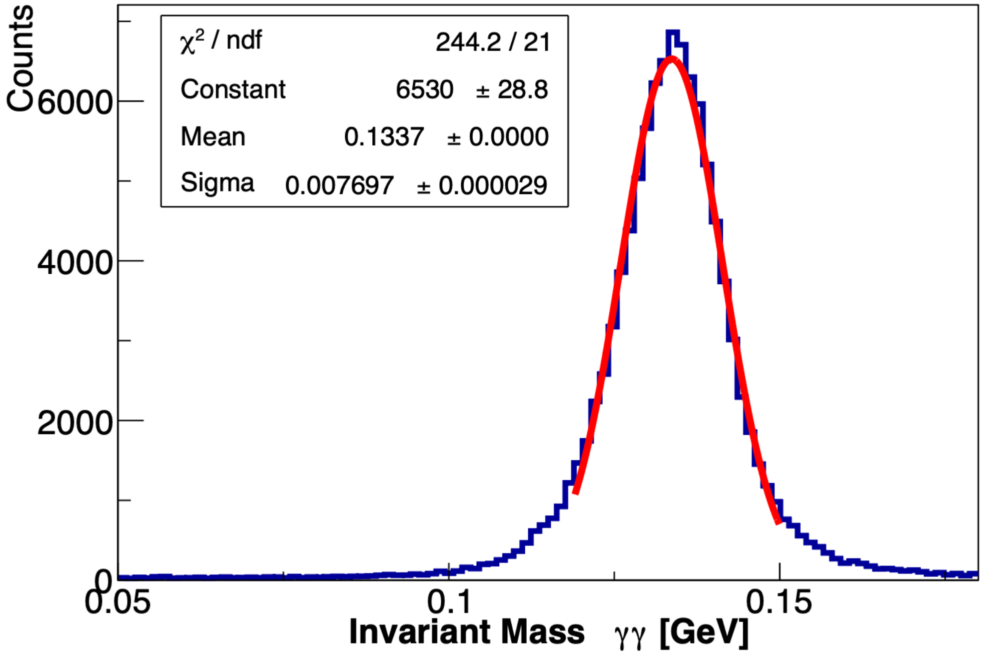

Exclusivity selection cuts

- Invariant mass.
- Missing energy.
- Missing masses.
- Missing transverse momenta.
- Angle between measured and reconstructed pion.

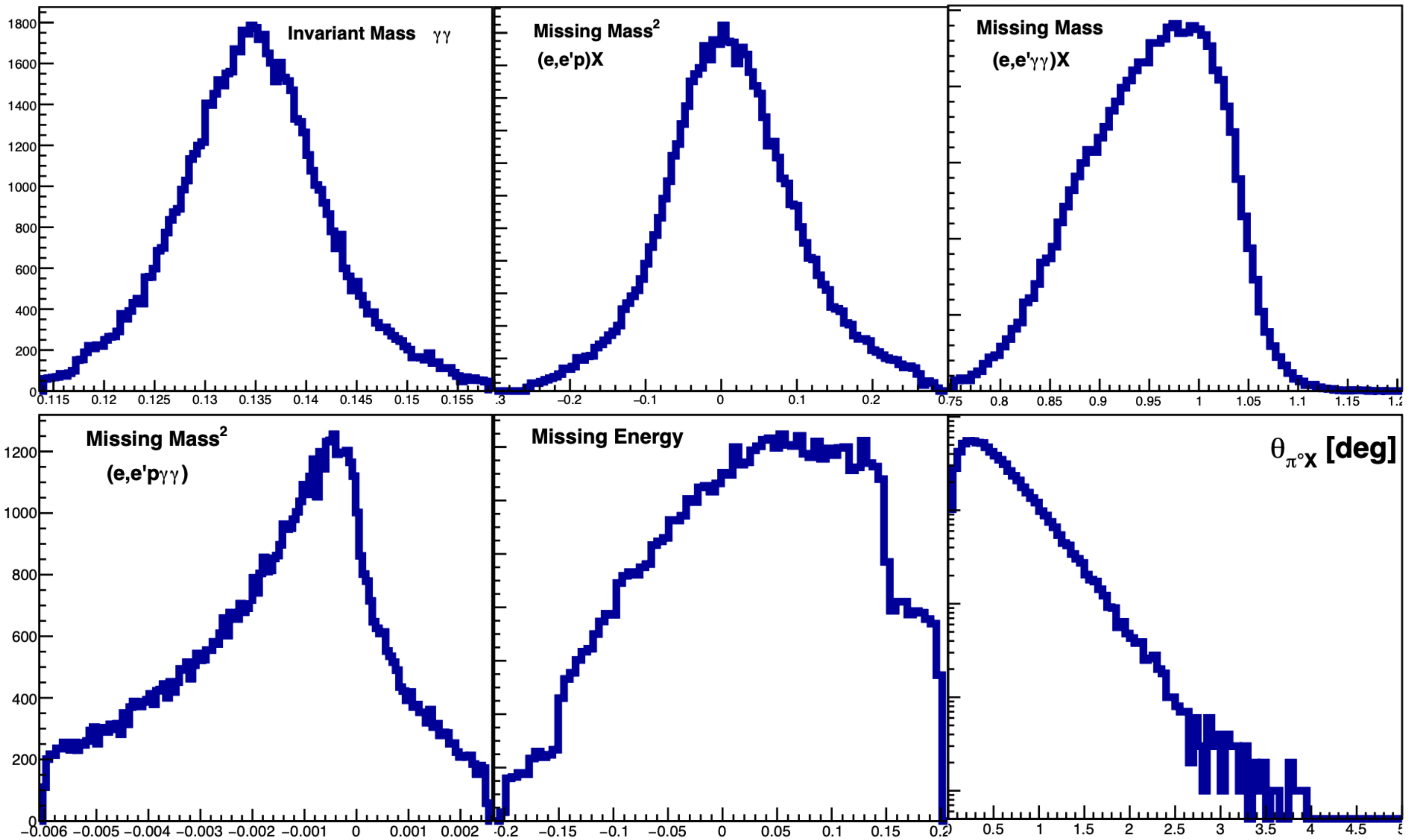

- $0.096 < M_{\gamma\gamma} < 0.168$ GeV$/c^2$,
- $|MM^2_{e'p'\pi^0}| < 0.002$ GeV^2,
- $-0.2 < ME_{e'p'\pi^0} < 0.15$ GeV,
- $MP_{T,e'p'\pi^0} < 0.2$ GeV.

Simulation - Data comparison

Use of “aao” generator

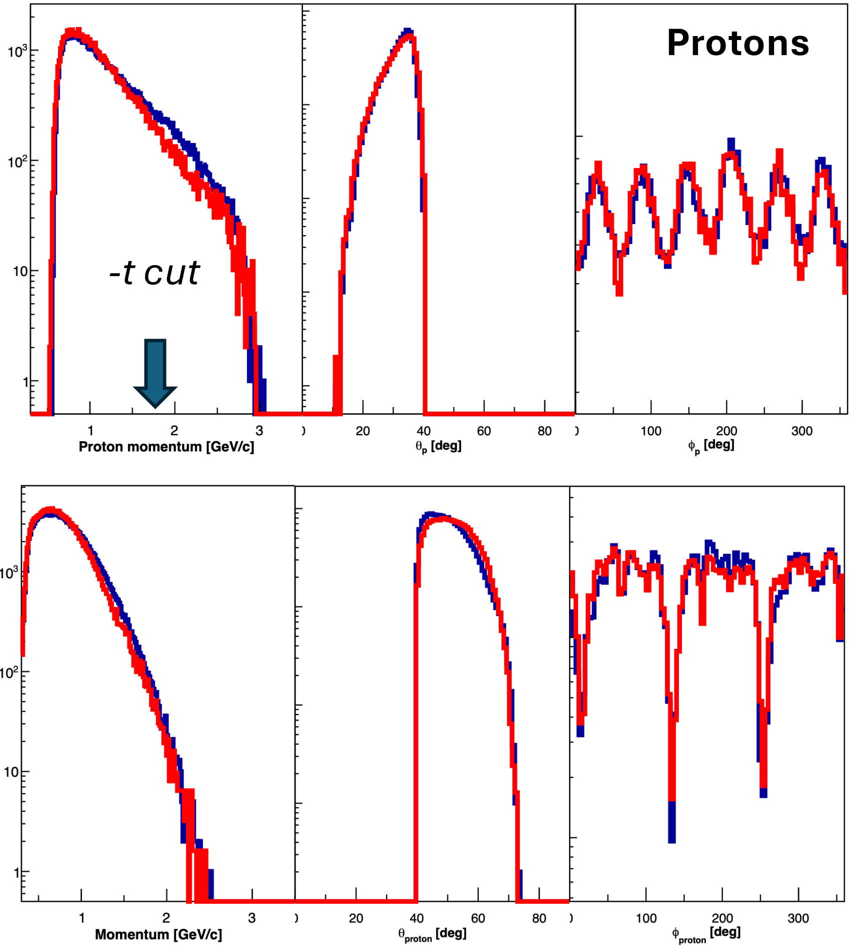

Electrons

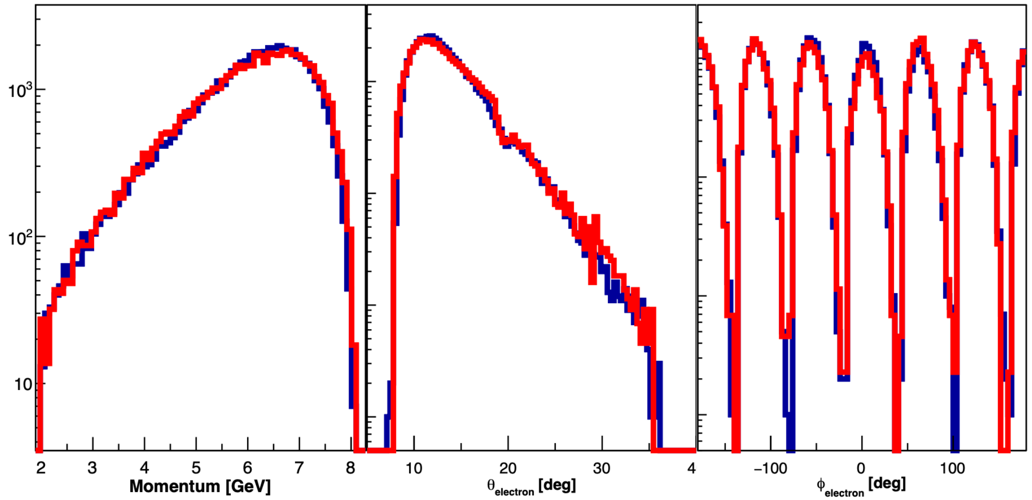

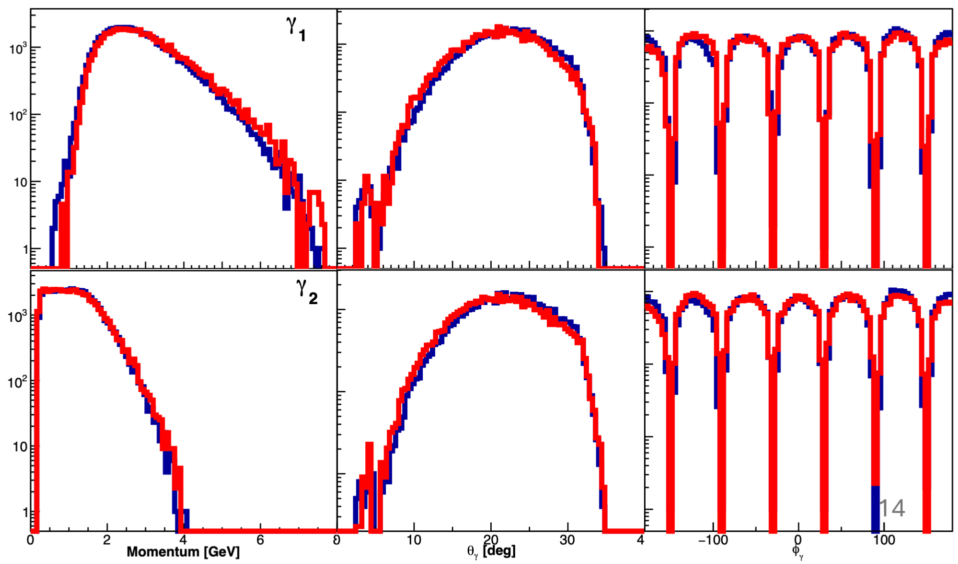

Additional smearing for proton (simulation after GEMC)

Smearing on protons:

- Momenta and angles.
- Topology dependent.

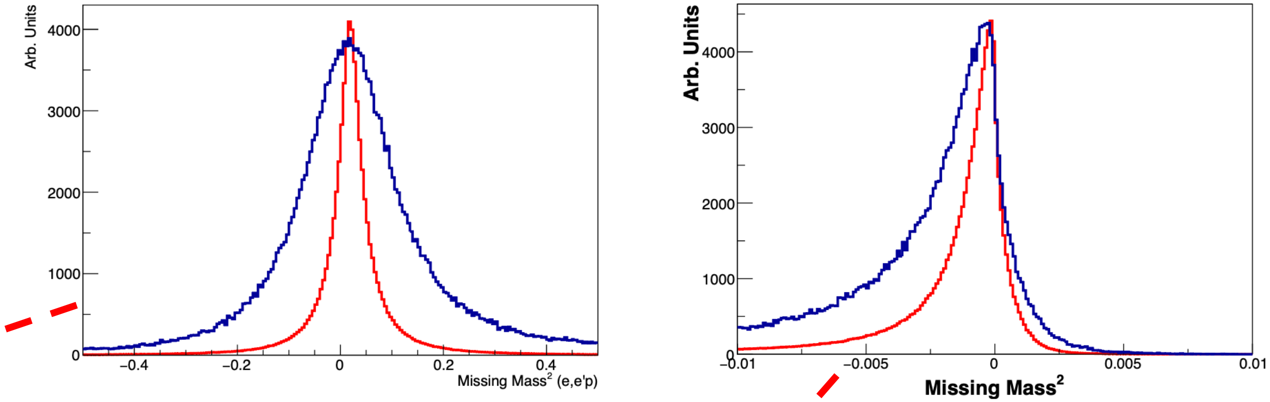

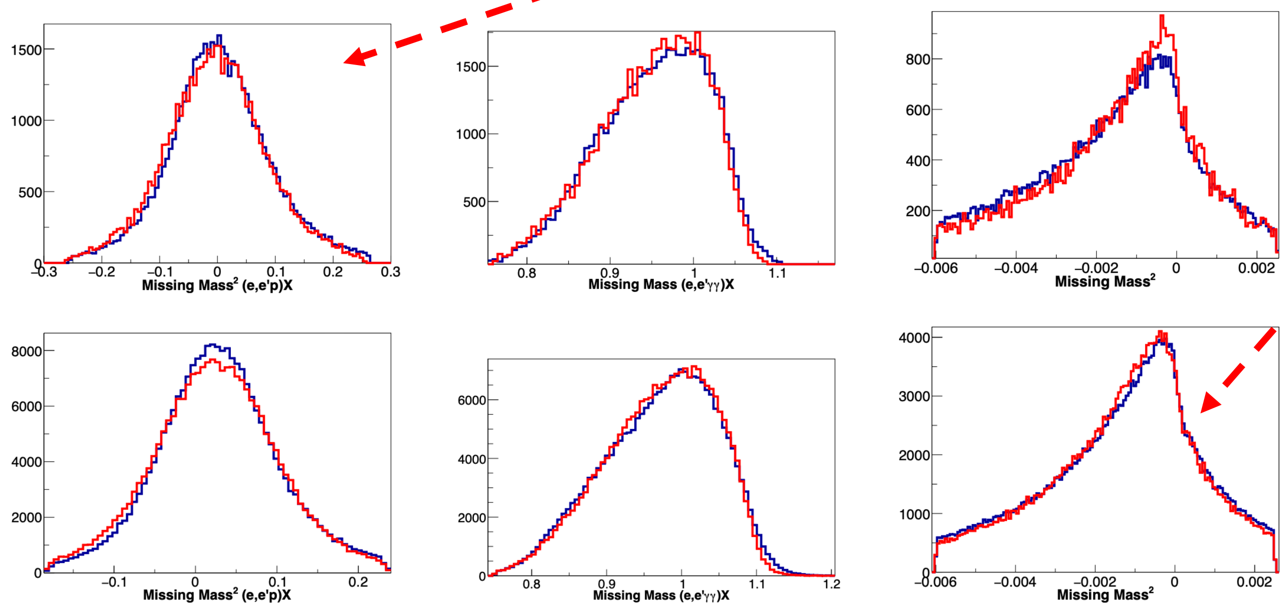

Acceptance correction studies

Simulation provides a tool to extract acceptance corrections factors. Done for each 4D bin.

Inbending configuration

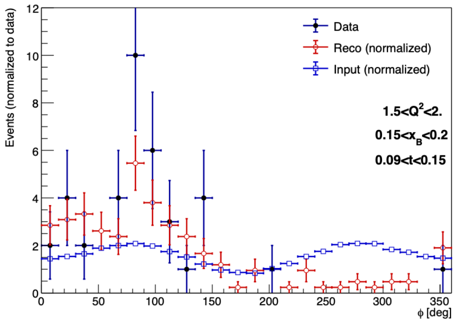

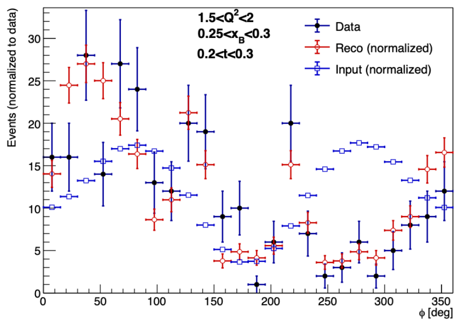

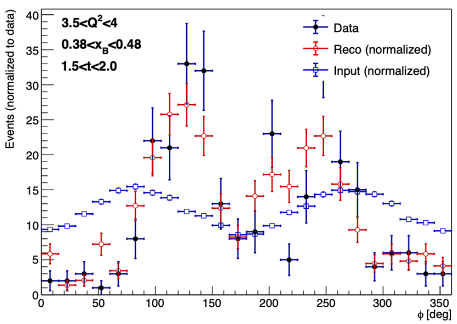

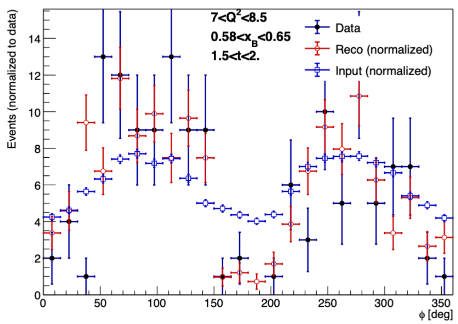

Oubending configuration

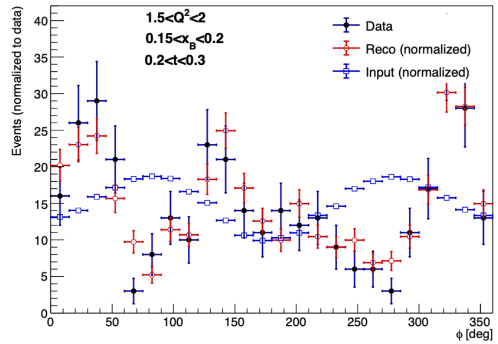

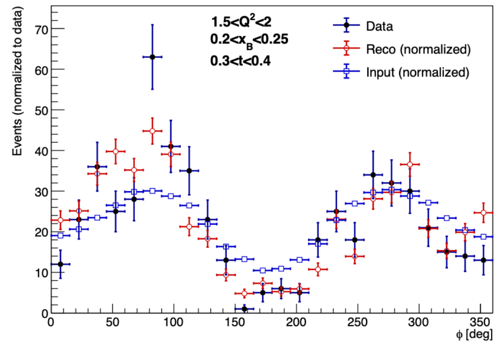

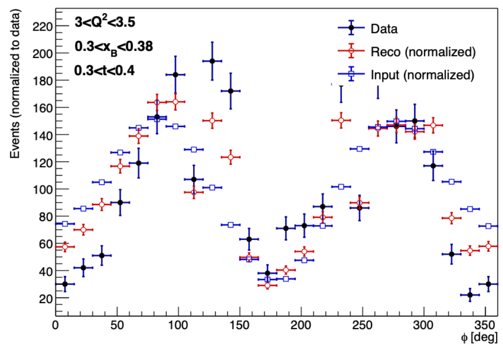

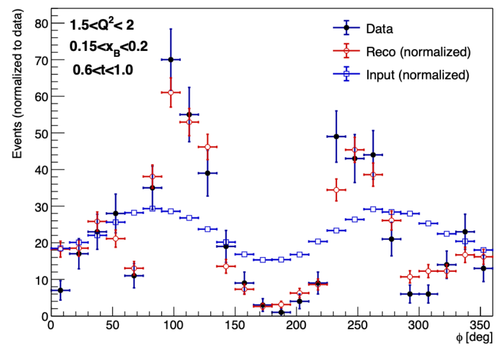

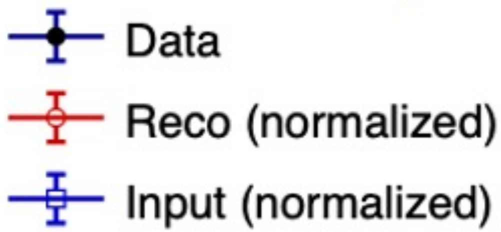

Comparison between inbending and outbending

inbending (black) / outbending (red)

All exclusivity cuts.

Normalized to the integrated luminosity.

No additional normalization between inbending and outbening

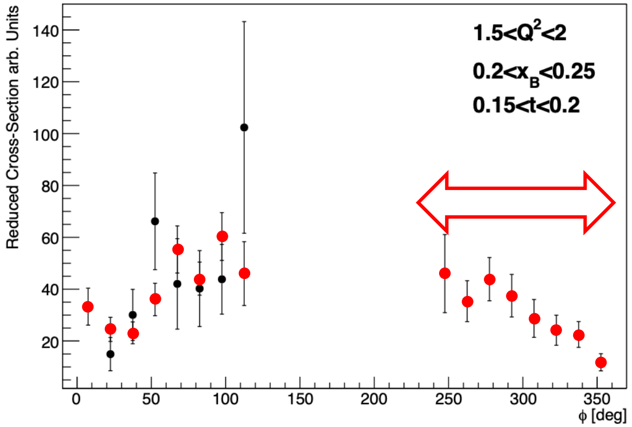

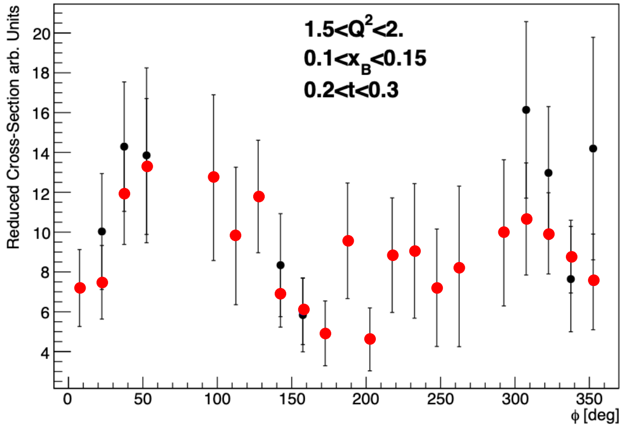

Combination between two configuration:

Weigthed average for each point

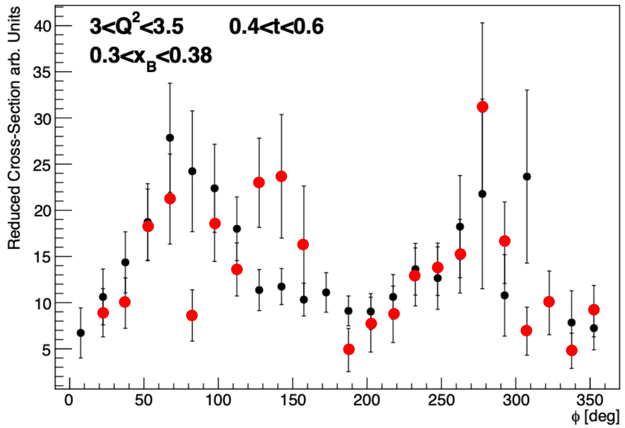

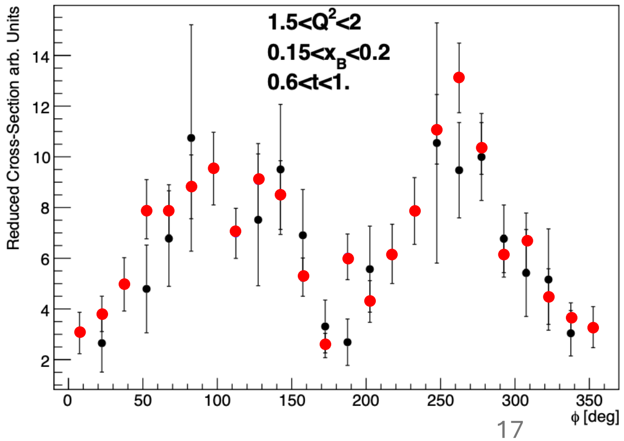

Difference in the central values of $Q^2, x_B, -t, \epsilon$

Systematic uncertainty limited up to 4%
The outliers are due to bins with limited coverage in phi angle

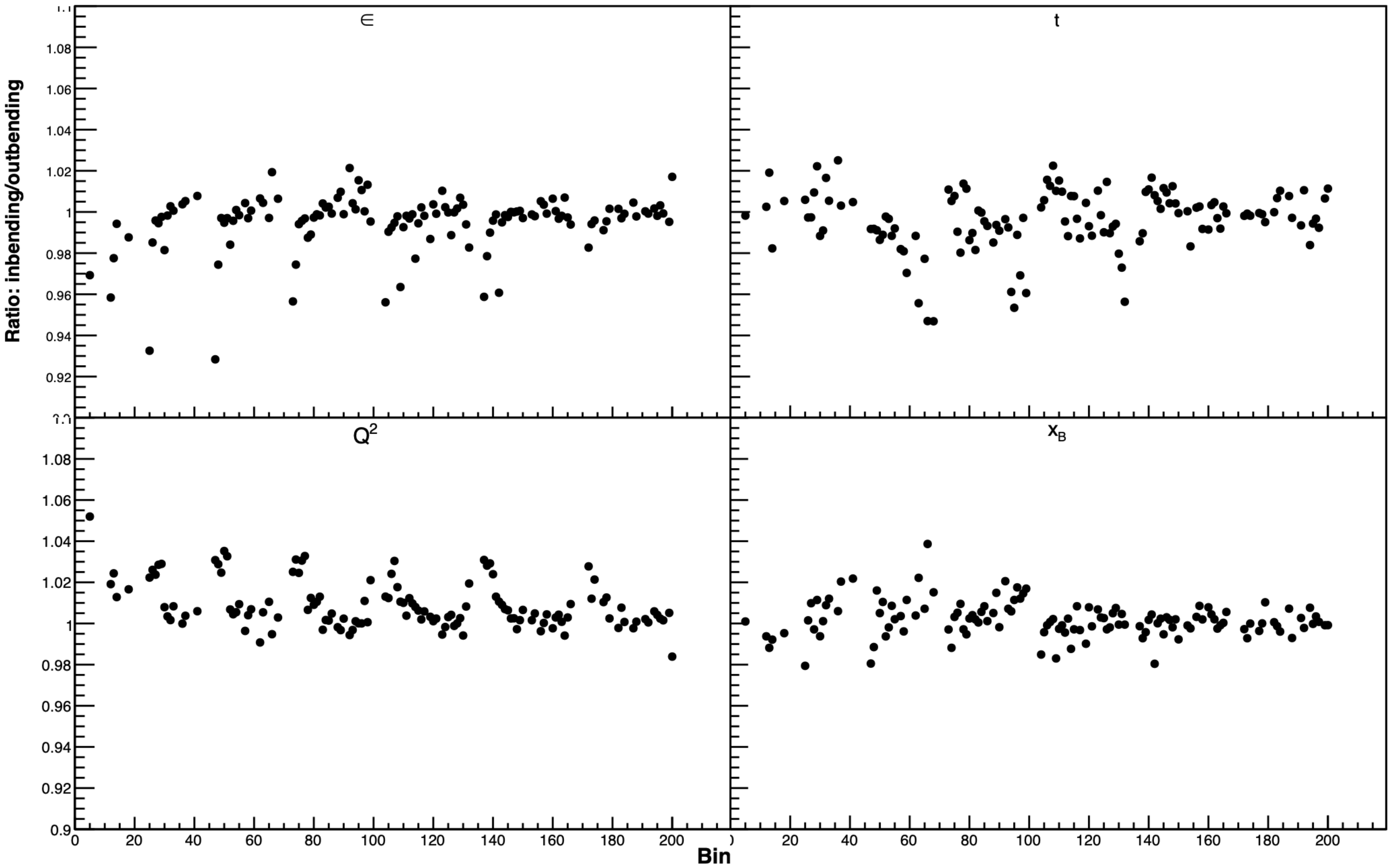

Phase space binning

Optimization: statistics and future comparison (specifically, clas6)

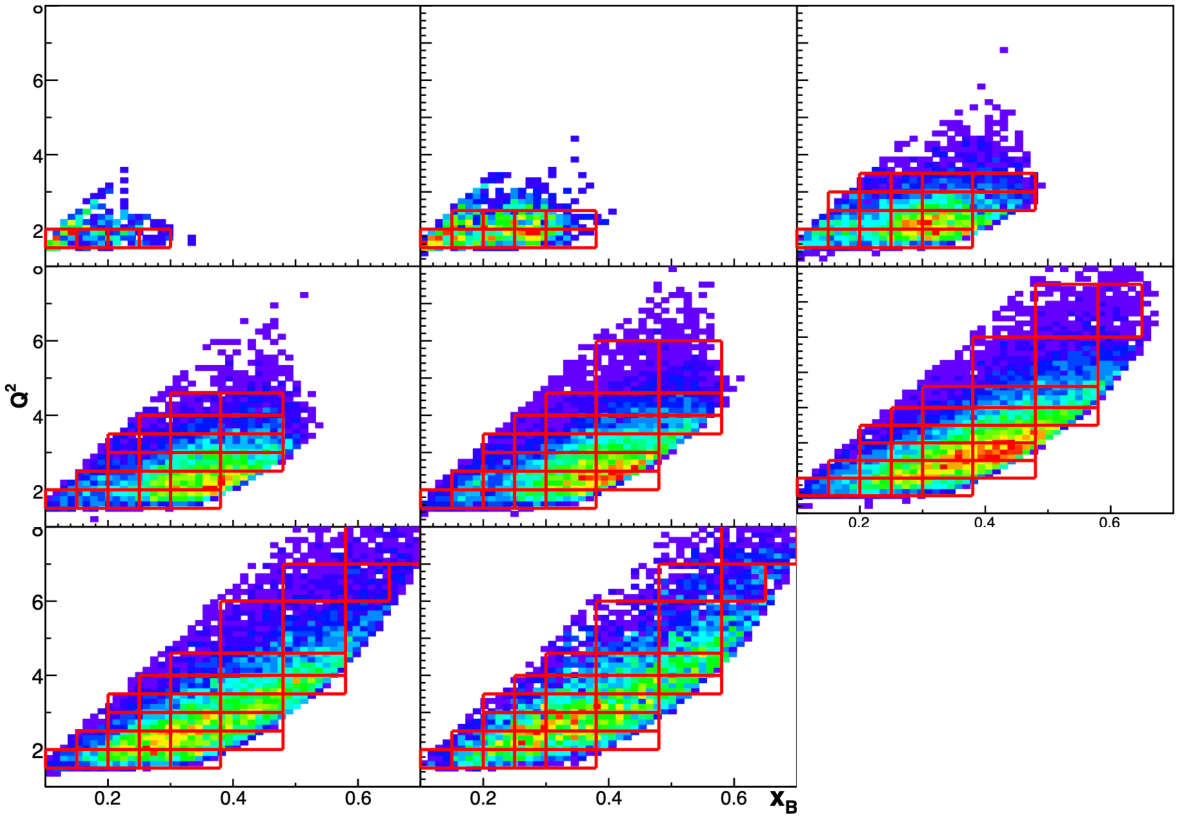

Min x_B	Max x_B
0.1	0.15
0.15	0.2
0.2	0.25
0.25	0.3
0.3	0.38
0.38	0.48
0.48	0.58
0.58	0.65

Min Q^2 [GeV^2]	Max Q^2 [GeV^2]
1.0	1.5
1.5	2.0
2.0	2.5
2.5	3.0
3.0	3.5
3.5	4.0
4.0	4.6
4.6	6.0
6.0	7.0
7.0	8.5

Min $-t$ [GeV^2]	Max $-t$ [GeV^2]
0.09	0.15
0.15	0.20
0.20	0.30
0.30	0.40
0.40	0.60
0.60	1.00
1.00	1.50
1.50	2.00

Extraction of structure functions

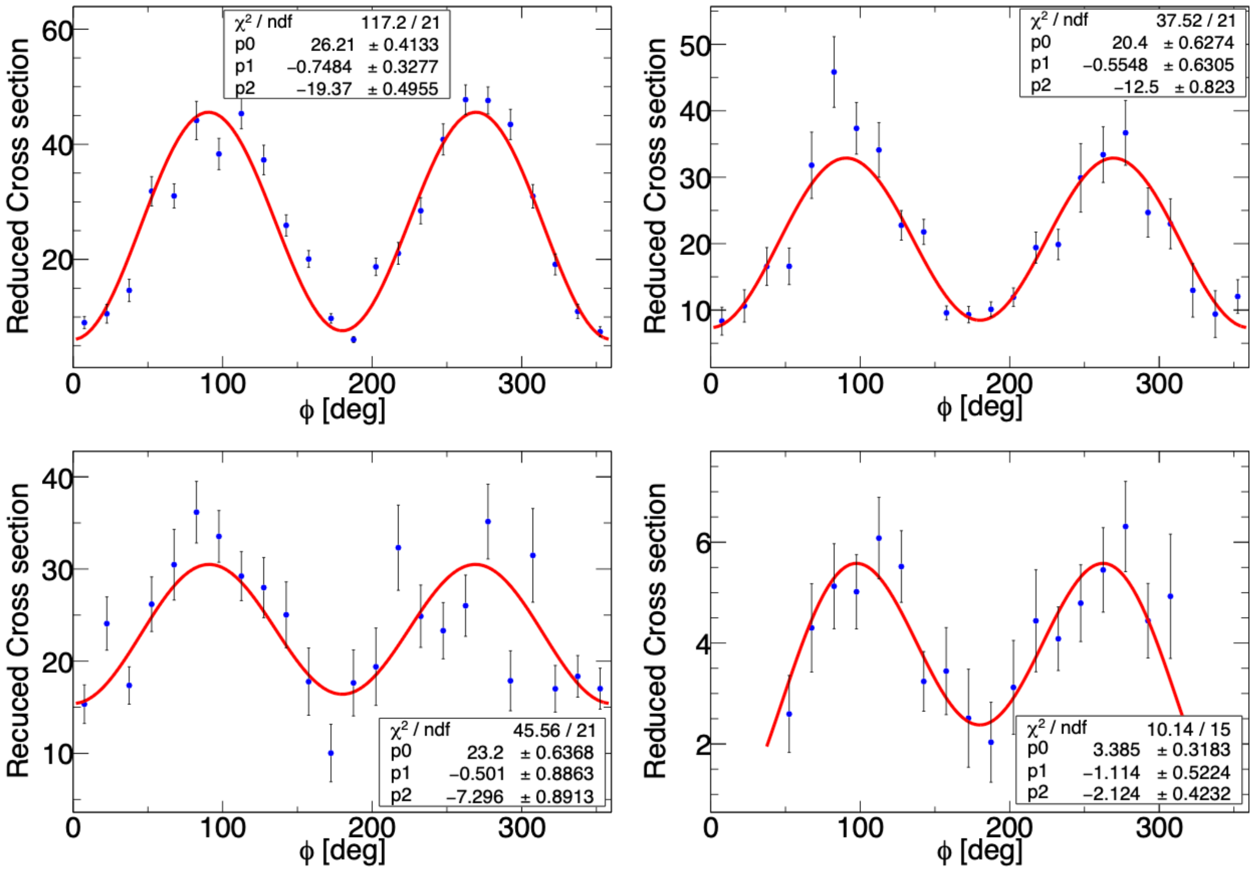

Empirical fit

$$\frac{d^2\sigma}{dt\,d\phi_\pi} = \frac{1}{2\pi}\boxed{\left[\left(\frac{d\sigma_T}{dt} + \epsilon\frac{d\sigma_L}{dt}\right)\right.} + \epsilon\cos 2\phi_\pi \boxed{\frac{d\sigma_{TT}}{dt}} + \sqrt{2\epsilon(1+\epsilon)}\cos\phi_\pi \boxed{\left.\frac{d\sigma_{LT}}{dt}\right]}$$

Low $-t$ range:

$Q^2 = 2$

$0.09 < -t < 0.15\ GeV^2$

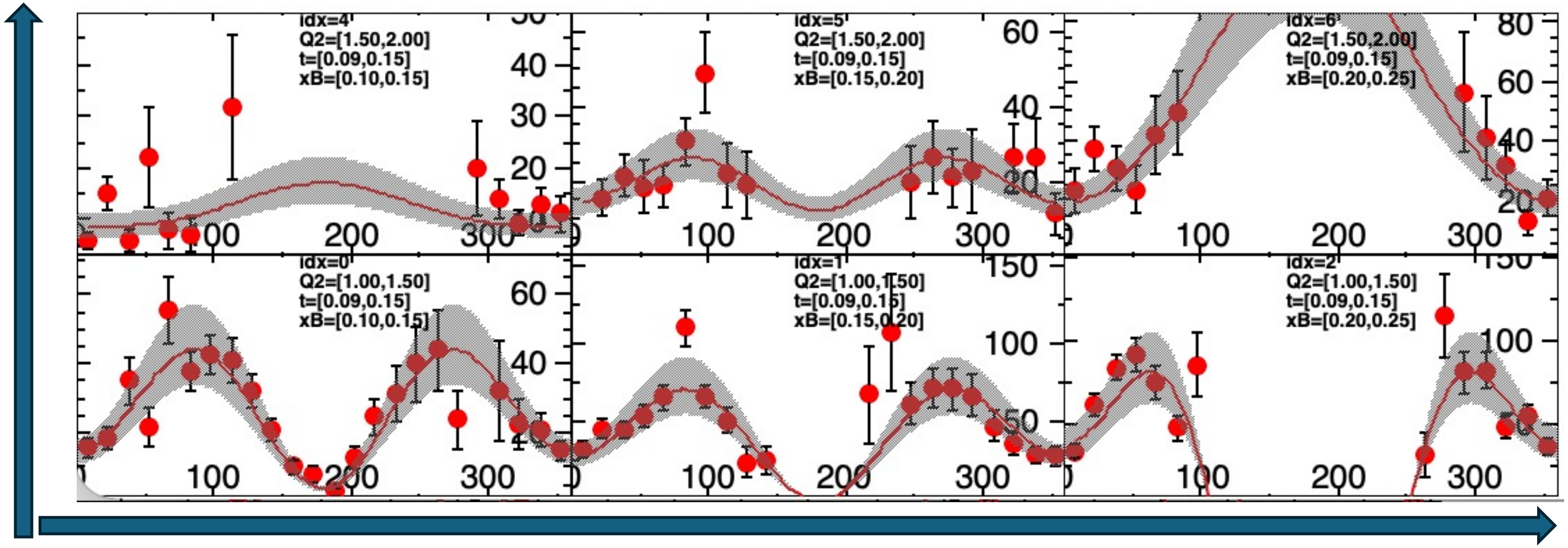

$Q^2 = 1$

$0.1 < x_B < 0.25$

Red line: empicical fit.

Gray area: normalization uncertainty.

High $-t$ bin

$1.5 < -t < 2\ GeV^2$

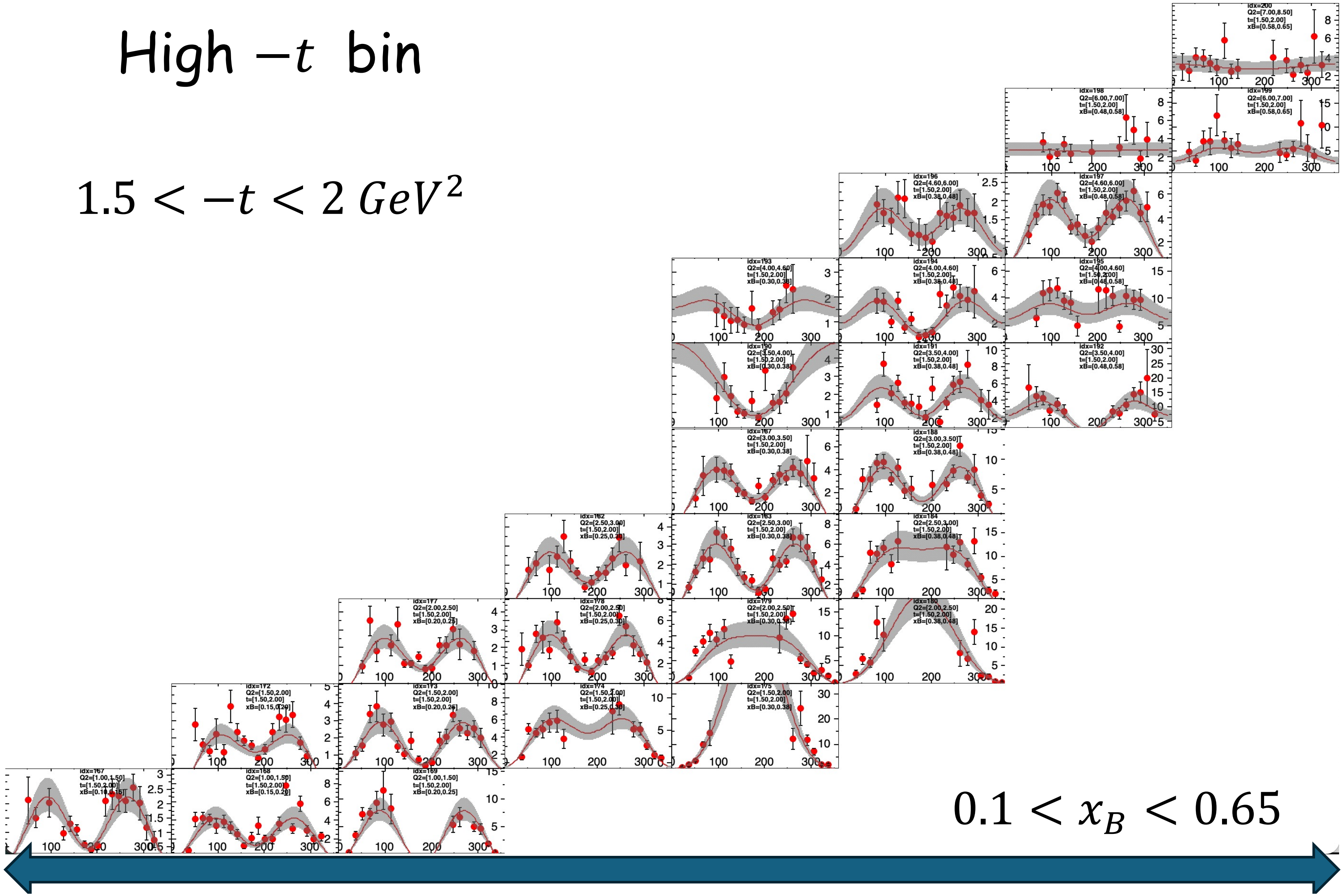

$0.1 < x_B < 0.65$

$Q^2 = 8.5$

$Q^2 = 1$

Global normalization

We scaled the cross-section results by **1.3** in both inbending and outbending data sets.

- ❖ Recent approved DVCS analysis from RGA

  Simulated yields were reweighted to match data
  → decreased acceptance → cross-section increase

- ❖ A recent J/ψ photoproduction analysis introduced about 20% global normalization to correct for similar detector-related effects.

Uncertainty budget

Source	Average Value	Range
Bin-by-bin uncertainties		
Fiducial cuts / PID	4%	1–15%
Exclusivity cuts	4%	1–10%
Momentum corrections	3%	1–14%
Simulation/data smearing	3%	2–5%
Acceptance corrections	3%	2–10%
Inbending/Oubending merging	8%	
Radiative corrections	3.5%	1–17%
Combined (quadrature)	$\sim 12\%$	
Overall scale uncertainties		
Integrated luminosity	2.5%	2–3%
$\pi^0 \to \gamma\gamma$ branching ratio	$< 0.1\%$	negligible
Normalization factor (DAQ live-time, trigger)	3%	2–3%
Total scale uncertainty	**4%**	3–5%
Total scaling factor	**1.3**	

t-Dependence and Impact Parameter Interpretation

$$\frac{d\sigma_U}{dt} = A\, e^{-B|t|}$$

$$\langle b_\perp^2 \rangle \;\simeq\; B$$

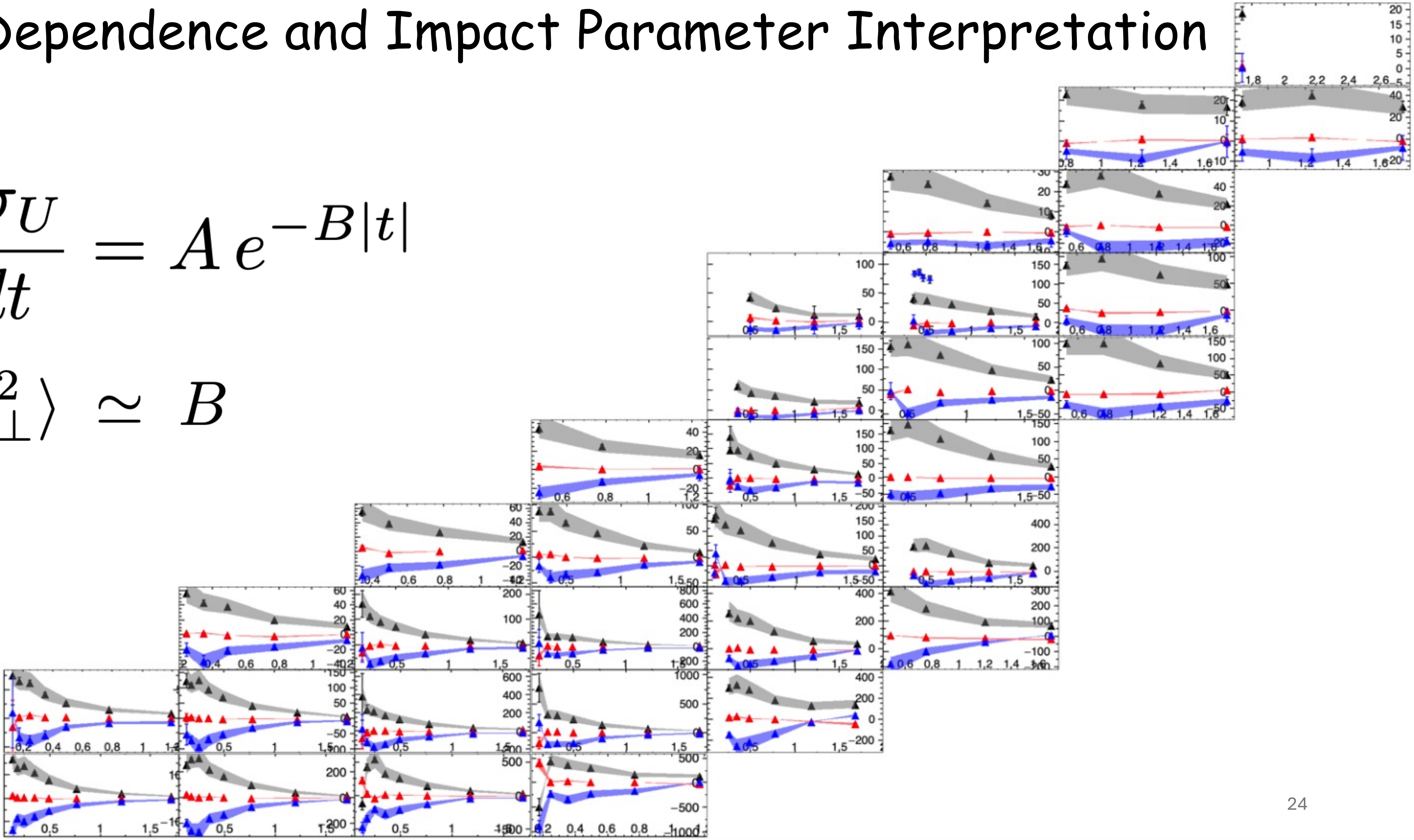

$$\frac{d\sigma_U}{dt} = A\,e^{-B|t|}$$

$$\langle b_\perp^2 \rangle \simeq B$$

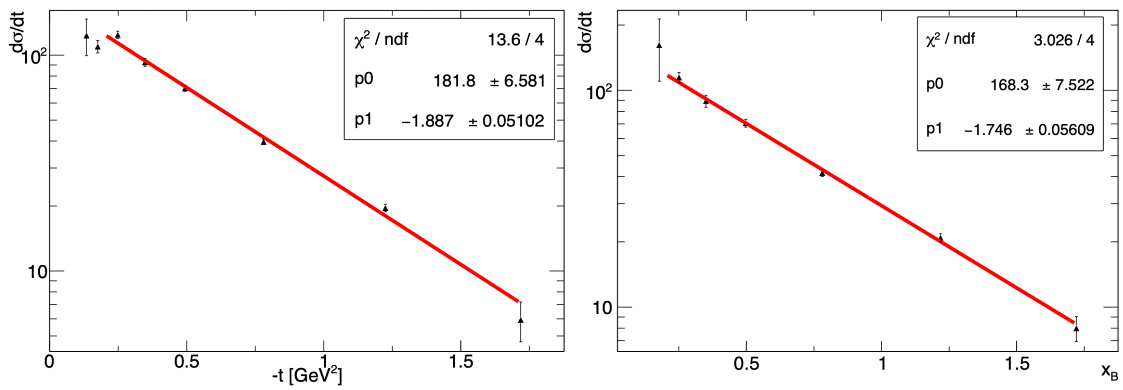

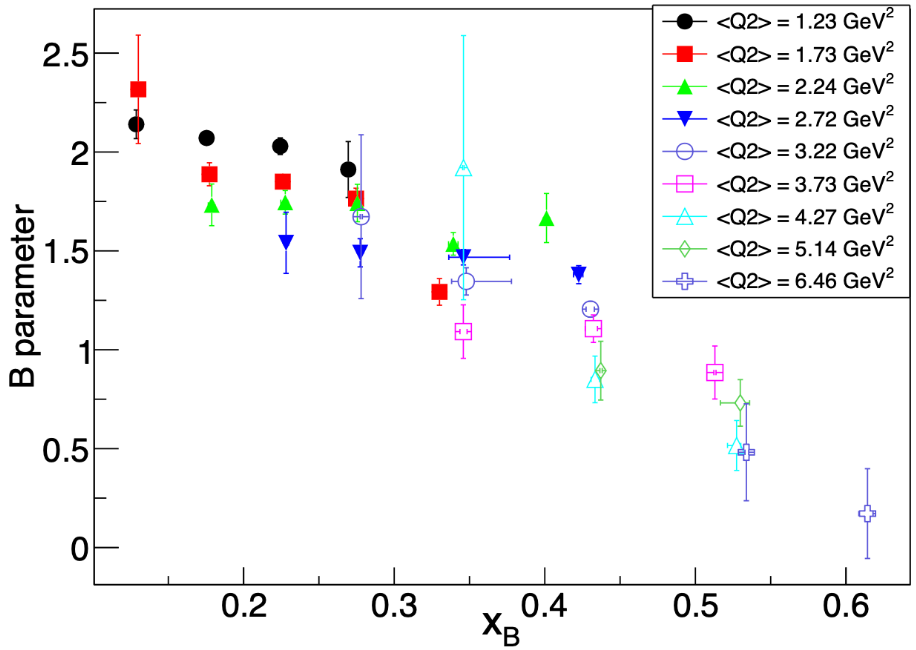

$-t$ dependence includes contribution form two GPDs

Physical interpretation requires data from neutron and eta meson.

Summary:

- The study of deeply virtual exclusive pseudoscalar meson production uniquely connected with the transversity GPDs.
- Current data set provide wide phase space coverage over many kinematical bins (~ 160 bins).
- Enables study of the dynamic as function of Q^2, x_B and $-t$ that in turn related to odd GPDs.
- Systematic studies show stability of the structure function.
- Main contribution to the uncertainty is a global normalization.
  - ❖ Dynamic behavior of SF is less sensitive to global normalization.